

A Circumbinary Planet in Orbit Around the Short-Period White-Dwarf Eclipsing Binary RR Cae

Qian S.-B.^{1,2,3}, Liu L.^{1,2,3}, Zhu L.-Y.^{1,2}, Dai Z.-B.^{1,2}, Fernández Lajús, E.^{4,5},
and Baume G. L.⁴

¹*National Astronomical Observatories/Yunnan Observatory, Chinese Academy of Sciences, P.O. Box 110, 650011 Kunming, P. R. China (qsb@ynao.ac.cn)*

²*Key laboratory of the structure and evolution of celestial objects, Chinese Academy of Sciences, P.O. Box 110, 650011 Kunming, P. R. China*

³*Graduate University of the Chinese Academy of Sciences, 100049 Beijing, P. R. China Yuquan Road 19#, Sijingshang Block, 100049 Beijing City, P. R. China*

⁴*Facultad de Ciencias Astronómicas y Geofísicas, Universidad Nacional de La Plata, 1900 La Plata, Buenos Aires, Argentina*

⁵*Instituto de Astrofísica de La Plata (CCT La plata - CONICET/UNLP), Argentina*

ABSTRACT

By using six new determined mid-eclipse times together with those collected from the literature, we found that the Observed-Calculated (O-C) curve of RR Cae shows a cyclic change with a period of 11.9 years and an amplitude of 14.3 s, while it undergoes an upward parabolic variation (revealing a long-term period increase at a rate of $\dot{P} = +4.18(\pm 0.20) \times 10^{-12}$). The cyclic change was analyzed for the light-travel time effect that arises from the gravitational influence of a third companion. The mass of the third body was determined to be $M_3 \sin i' = 4.2(\pm 0.4) M_{Jup}$ suggesting that it is a circumbinary giant planet when its orbital inclination is larger than 17.6° . The orbital separation of the circumbinary planet from the central eclipsing binary is about $5.3(\pm 0.6)$ AU. The period increase is opposite to the changes caused by angular momentum loss via magnetic braking or/and gravitational radiation, nor can it be explained by the mass transfer between both components because of its detached configuration. These indicate that the observed upward parabolic change is only a part of a long-period (longer than 26.3 years) cyclic variation, which may reveal the presence of another giant circumbinary planet in a wide orbit.

Key words: Stars: binaries : close – Stars: binaries : eclipsing – Stars: individuals (RR Cae) – Stars: white dwarfs – Stars: planetary system

1 INTRODUCTION

RR Cae is one of a few double-lined eclipsing binaries (e.g., V471 Tau, QS Vir, RXJ2130.6+4710, and RR Cae) containing white dwarfs where the masses and radii of both component stars can be determined accurately (e.g., O’Brien et al., 2001; O’Donoghue et al., 2003; Maxted et al., 2004, 2007). It was discovered to be an eclipsing binary by Krzeminski (1984) in which the cool white dwarf component is eclipsed by an M-type dwarf companion every 7.3 h. The amplitude of the radial velocity (of the dMe star) throughout the orbit was mentioned as 370 km/s. Bruch & Diaz (1998) published an R-band light curve and classified the spectral type of the red-dwarf companion as M5 V or M6 V. Further spectroscopy around the H_α line was presented by Bruch (1999) who derived a spectroscopic orbit for the M-dwarf and determined absolute parameters of the binary system. The mass

of the M-type dwarf was estimated as $0.09 M_\odot$ by Bruch & Diaz (1998) and Bruch (1999), which was much lower than expected given its spectral type. Several narrow absorption lines of neutral metals, e.g., Al I, Fe I and Mg I, were found by Zuckerman et al. (2003) with Keck telescope HIRES echelle observations, which were thought to have been accreted onto the surface of the white dwarf from the M-dwarf. A more detailed photometric and spectroscopic investigation was recently presented by Maxted et al. (2007). They showed that RR Cae is a detached binary containing a cool white dwarf primary with a mass of $0.44 M_\odot$ and an M_4 -type secondary with a mass of $0.182 M_\odot$.

Searching for planetary companions to short-period white dwarf binaries will shed light on the formation and evolution of planets, as well as provide insight into the ultimate fate of planets and the interaction between planets and evolved stars. Because of the very small size of the white

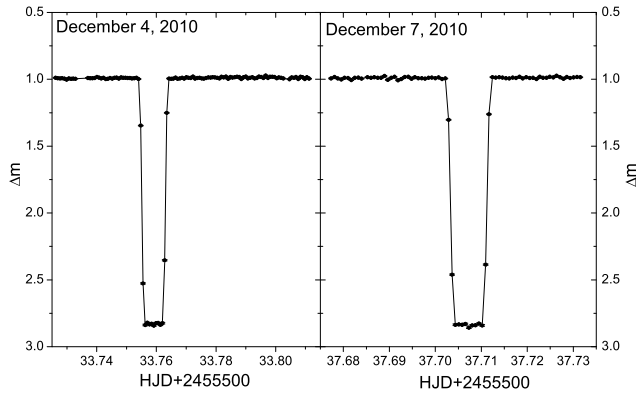


Figure 1. Light curves of RR Cae in V band obtained by using the 2.15-m Jorge Sahade telescope on December 4 and 7, 2010. The coordinates of the comparison star are: $\alpha_{2000} = 04^h 20^m 46.1^s$ and $\delta_{2000} = -48^\circ 41' 46.8''$, while those of the check star are: $\alpha_{2000} = 04^h 20^m 41.2^s$ and $\delta_{2000} = -48^\circ 37' 35.4''$.

dwarfs, eclipse times of this type of binary system can be determined with a high precision, and very small-amplitude variations in the orbital periods could be detected by analyzing the observed-calculated (O-C) diagrams. Therefore, they are the most promising targets to search for circumbinary brown dwarfs and planets by analyzing the light-travel-time effect. To date, a few substellar companions to eclipsing white-dwarf binaries were found by using this method, such as V471 Tau (e.g., Guinan & Ribas 2001), DP Leo (Qian et al. 2010a; Beuermann et al. 2011), QS Vir (Qian et al. 2010b, Almeida & Jablonski 2011), NN Ser (Qian et al. 2009; Beuermann et al. 2011), and HU Aqr (Qian et al. 2011). In this letter, by including 6 new mid-eclipse times, the variations of the O-C curve of RR Cae were analyzed. Our results suggest that there is a circumbinary giant planet orbiting the eclipsing binary, and there is some evidence for a second, more distant companion.

2 NEW OBSERVATIONS AND THE CHANGES OF THE O-C CURVE

The white dwarf-red-dwarf eclipsing binary, RR Cae, was monitored on December 4 and 7, 2010 with Roper Scientific, Versarray 1300B camera, with a thinned EEV CCD36-40 de 1340×1300 pix CCD chip, attached to the 2.15-m Jorge Sahade telescope at Complejo Astronomico El Leoncito (CASLEO), San Juan, Argentina. During the observation, V filter was used and an exposure time for each CCD im-

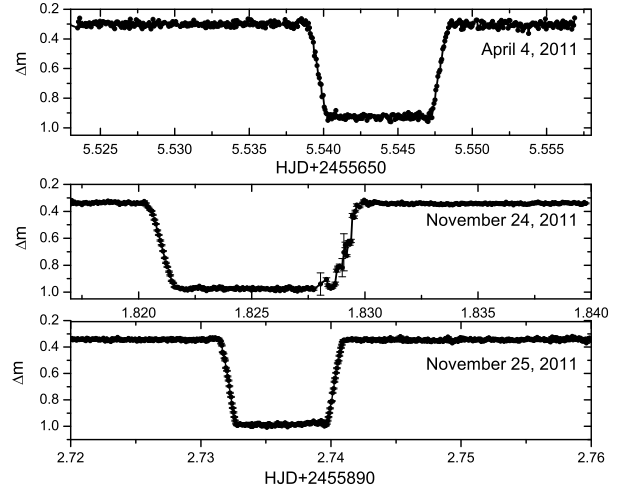


Figure 2. Three white-light eclipse profiles of the short-period eclipsing binary RR Cae observed in April and December, 2011.

age was adopted as 50 s. The clock of the control computer operating the VersArray 1300B CCD camera is calibrated against UTC time by the GPS receiver's clock. Two nearby stars that have similar brightness in the same field of view of the telescope were chosen as the comparison star and the check star, respectively. All images were reduced by using PHOT (measure magnitudes for a list of stars) of the aperture photometry package of IRAF. The corresponding light curves are displayed in Fig. 1; the eclipse depth is about 1.84 magnitudes.

To get more mid-eclipse times of the binary star, we re-observed it in April and November 2011. The exposure time for each CCD image was adopted as 2 s and no filters were used. Three eclipse profiles are shown in Fig. 2. As displayed in the figure, the time of the flat-bottomed minimum was estimated as 8.4 minutes. By using the midpoint times of steep ingress and egress of eclipse, we determined six mid-eclipse times which are listed in Table 1. Since Barycentric Dynamical Time (BJD) is a precise time system, during the analyzing we applied this time system. The HJD times were converted to BJD ones with the code of Stumpff (1980) and those mid-eclipse times in both the HJD and BJD are shown in Table 1.

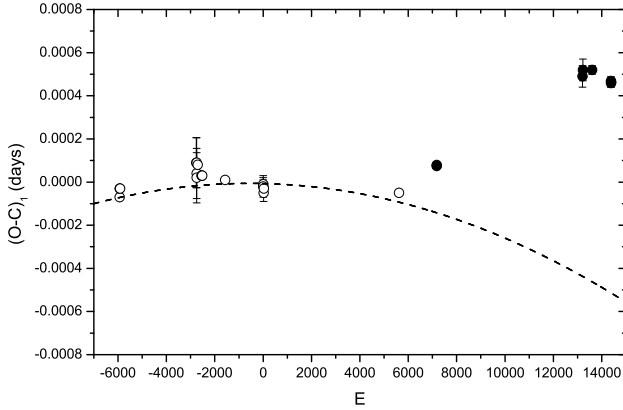
Times of mid-eclipse of RR Cae were published by a few authors (e.g., Krzeminski, 1984; Bruch & Diaz, 1998; Maxted et al., 2007; Parsons et al., 2010). The $(O - C)_1$ values of all available mid-eclipse times were calculated with the linear ephemeris derived by Maxted et al. (2007),

$$Min.I = BJD\,2451523.048567 + 0^d.3037036366 \times E, \quad (1)$$

where BJD 2451523.048567 is the initial epoch and

Table 1. New CCD times of light minimum of RR Cae.

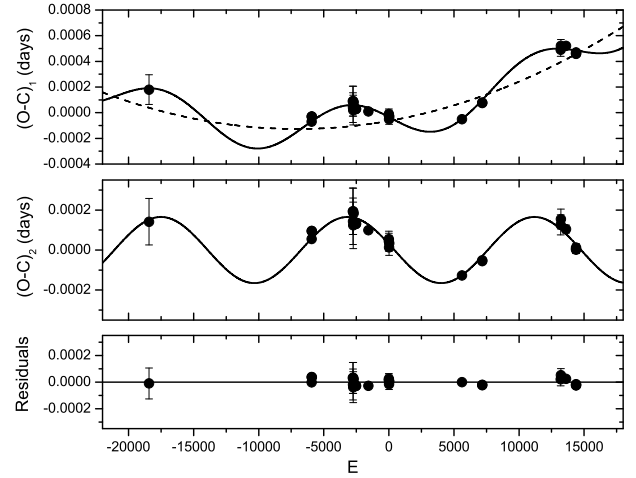
HJD (days)	BJD (days)	Errors (days)	Filters
2455533.75855	2455533.75931	± 0.00005	V
2455537.70673	2455537.70749	± 0.00005	V
2455655.54371	2455655.54447	± 0.00002	N
2455889.69915	2455889.69991	± 0.00002	N
2455891.82509	2455891.82585	± 0.00002	N
2455892.73619	2455892.73695	± 0.00002	N


Figure 3. Residuals from the linear ephemeris of Maxted et al. (2007). Open circles refers to the data published by Bruch & Diaz (1998) and by Maxted et al. (2007), while solid circles to the observations obtained by Parsons et al. (2010) and the present authors. The dashed line represents the quadratic fit derived by Maxted et al. (2007).

0.3037036366 days is the orbital period. The corresponding $(O - C)_1$ diagrams are shown in Figs. 3 and 4 along with the epoch number E . By removing the mid-eclipse time, BJD 2445927.91665, determined by Krzeminski (1984), Maxted et al. (2007) obtained the following quadratic ephemeris,

$$\begin{aligned} \text{Min.}I &= \text{BJD } 2451523.048560 + 0^d.3037036340 \\ &\quad - 2.27 \times 10^{-12} \times E^2, \end{aligned} \quad (2)$$

with their mid-eclipse times and those published by Bruch & Diaz (1998). The quadratic term in this ephemeris reveals a period decrease as a rate of $\dot{P}/P = -5 \times 10^{-12}$. However, as shown in Fig. 3, our data and those determined by Parsons et al. (2010) do not follow the general trend predicted by


Figure 4. A plot of the $(O - C)_1$ curve of RR Cae from the linear ephemeris of Maxted et al. (2007) is shown in the upper panel. The solid line in the panel refers to a combination of an upward parabolic variation and a cyclic change. The dashed line represents the upward parabolic variation that reveals a continuous increase in the orbital period. The $(O - C)_2$ values with respect to the quadratic part of Eq. (3) are displayed in the middle panel where a cyclic change is more clearly seen. After both the upward parabolic change and the cyclic variation were removed, the residuals are plotted in the lowest panel.

the quadratic ephemeris suggesting that the variation of the $(O - C)_1$ curve of RR Cae is very complex.

To fit the $(O - C)_1$ curve satisfactorily, a combination of an upward parabolic variation and a cyclic change are required (solid line in the upper panel in Fig. 4). A least-square solution of all available data leads to,

$$\begin{aligned} (O - C)_1 &= -0.000064(\pm 0.000005) \\ &\quad + 1.79(\pm 0.08) \times 10^{-8} \times E \\ &\quad + 1.27(\pm 0.06) \times 10^{-12} \times E^2 \\ &\quad + 0.000165(\pm 0.000013) \sin[0.^\circ 02590] \end{aligned}$$

$$(\pm 0.^\circ 00010) \times E + 169.2^\circ (\pm 0.8^\circ)], \quad (3)$$

which suggests a cyclic oscillation with a very small amplitude of 14.3 s and a period of 11.9 years. The quadratic term in Eq. (3) indicates a linear increase at a rate of $\dot{P} = +4.18(\pm 0.20) \times 10^{-12}$ s/s (or 1.3 s in about 10000 years). The dashed line in the upper panel of Fig. 4 refers to the linear period increase, while the solid one represents the combination of the linear increase and the cyclic change. The $(O - C)_2$ values with respect to the quadratic part Eq. (3) are displayed in the middle panel where a small-amplitude periodic variation can be seen more clearly. After both of the linear increase and the cyclic change were subtracted, the residuals are plotted in the lowest panel where no variations can be traced indicating that Eq. (3) describes the general trend of the $(O - C)_1$ curve well.

3 DISCUSSIONS AND CONCLUSIONS

As shown in the middle panel of Fig. 4, after the upward parabolic variation is subtracted from the $(O - C)_1$ curve, the $(O - C)_2$ residuals suggest that there is a cyclic variation with a period of 11.9 years. The cyclic change of the mid-eclipse times represent either true or apparent variations (e.g., caused by apsidal motion or the presence of a third body) in the orbital period. As for the true cyclic variation, it was usually attributed to the mechanism of Applegate (1992). In this mechanism, the changes in the internal constitution of the cool component star during the magnetic activity cycles result in the variation of the orbital period through spin-orbit coupling. However, the secondary of RR Cae is a fully convective M4-type star; Applegate's mechanism in such cool stars is generally too feeble to explain the observed amplitudes (e.g., Brinkworth et al. 2006). On the other hand, RR Cae is a short-period binary with an orbital period of 7.3 h, and the strong tidal interaction is expected to circularize the orbit efficiently. Apsidal motion cannot account for the cyclic variation in the mid-eclipse times. Therefore, the periodic change of the $(O - C)_2$ residuals can be plausibly explained as light-travel-time effect caused by the motion of the eclipsing binary via the presence of an invisible companion.

The sine-like variation of the $(O - C)_2$ curve in the middle of Fig. 4 suggests that the eccentricity of the orbit of the tertiary component is close to zero. The projected radius of the orbit of the eclipsing pair rotating around the barycenter of the triple system was computed with this equation,

$$a'_{12} \sin i' = A_3 \times c, \quad (4)$$

where A_3 is the amplitude of the O-C oscillation and c is the speed of light, i.e., $a'_{12} \sin i' = 0.029(\pm 0.002)$ AU (1 AU is the mean distance between the earth and the Sun). Then, by using the absolute parameters determined by Maxted et al. (2007), a calculation with the following equation,

$$f(m) = \frac{4\pi^2}{GP_3^2} \times (a'_{12} \sin i')^3 = \frac{(M_3 \sin i')^3}{(M_1 + M_2 + M_3)^2}, \quad (5)$$

where G and P_3 are the gravitational constant and the period of the $(O - C)_2$ oscillation, yields the mass function and the mass of the tertiary companion as: $f(m) = 1.7(\pm 0.3) \times 10^{-7} M_\odot$ and $M_3 \sin i' = 0.00401(\pm 0.00037) M_\odot = 4.2(\pm 0.4) M_{Jup}$, respectively. If the orbital inclination of the third

Table 2. The derived planetary parameters in RR Cae.

Parameters	Value and uncertainty
Period (P_3)	11.9 \pm 0.1 yr
Eccentricity (e_3)	0.0
Amplitude (K_3)	14.3 \pm 1.1 s
$f(m)$	$1.7(\pm 0.3) \times 10^{-7} M_\odot$
$M_3 \sin i'$	$4.2 \pm 0.4 M_{Jup}$
$a_3(\sin i' = 90^\circ)$	$5.3(\pm 0.6)$ AU
χ^2	1.03
RMS of the least square fit	3.05×10^{-5} days

body is larger than 17.6° , the mass of the tertiary component corresponds to: $M_3 \leq 0.014 M_\odot$, and it should be an extrasolar planet. Therefore, with 95.3% probability, the third body is a giant planet (by assuming a random distribution of orbital plane inclination). The parameters of the circumbinary giant planet are shown in Table 2. When the orbital inclination equals 90° , the orbital distance between the circumbinary planet and the central binary is about $5.3(\pm 0.6)$ AU.

It is interesting to point out that the proposed planet has a period of 11.9 years and an eccentricity consistent with zero, which are essentially identical to the period and eccentricity of Jupiter ($P = 11.86$ years, $e = 0.05$). This raises the question as to whether the gravitational influence of Jupiter has been properly accounted for in the timing calculations. During the analysis, we used Barycentric Dynamical Time, which considers the influence of all planets. The light-travel time amplitude induced by the orbit of Jupiter about the Solar System barycentre is 2.48 seconds. Thus, an error omitting Jupiter's influence cannot have caused the observed cyclic signal with an amplitude of 14.3 seconds.

The upward parabolic variation in the $(O - C)_1$ curve indicates that the period of RR Cae is increasing continuously at a rate of $\dot{P} = +4.18(\pm 0.20) \times 10^{-12}$ s/s. Since RR Cae is a detached binary system where both components are in the critical Roche lobes, no lobe-filling mass transfers occur between both components. Moreover, the angular momentum loss caused by gravitational radiation or/and magnetic braking should produce a decrease in the orbital period. Therefore, neither mass transfer nor angular momentum loss can explain the period increase of RR Cae. All of these suggest that the observed upward parabola in the $(O - C)_1$ curve may be an apparent variation in the orbital period due to the influence of an additional orbiting body. As in the cases of the eclipsing polar HU Aqr (Qian et al. 2011) and the sdB-type eclipsing binary NY Vir (Qian et al. 2012), it may be only a part of a long-period (longer than 26.3 years) cyclic change, possibly revealing the presence of another circumbinary planet in a wider orbit. Some authors (e.g., Horner et al. 2011; Wittenmyer et al. 2012) proposed that the serious problem for the presence of the fourth body is the dynamical stability of the circumbinary planetary system. However, dynamical simulations by Hinse et al. (2011) suggested a family of stable orbital solutions, though for shorter timescales than tested by Horner et al. (2011).

If the cyclic variations in the O-C curve of RR Cae are really caused by the light-travel time effects via the presence

of circumbinary planets, they should be strictly periodic. To check the existence of the planetary system, more mid-eclipse times are needed in the future. Moreover, as pointed out by Qian et al. (2012), at the maximum points of the cyclic O-C changes, RR Cae should be at the farthest position of the orbit, while the circumbinary planets are closest to the observer. If the tertiary companion is coplanar to the central eclipsing binary, the circumbinary planet should be in the light of the binary system and transit the binary component stars. Therefore, searching for the transits of the binary components by the circumbinary planets at the O-C maxima can ascertain the presence of the planetary system. However, the possibility of transits is very low (0.026% by assuming a radius of $0.3 R_{\odot}$ for the M dwarf stars). Recently, a Saturn-like planet transiting the M-type components in the eclipsing binary Kepler-16 was reported by Doyle et al. (2011), which provides the first direct evidence for the presence of a circumbinary planet.

ACKNOWLEDGMENTS

This work is partly supported by Chinese Natural Science Foundation (No.11133007, No.10973037, No.10903026, and No.11003040) and by the West Light Foundation of the Chinese Academy of Sciences. New CCD photometric observations of RR Cae were obtained with the 2.15-m "Jorge Sade" telescope.

REFERENCES

- Almeida, L. A. & Jablonski, F., 2011, IAUS 276, 495
- Applegate, J. H., 1992, ApJ 385, 621
- Beuermann, K., Buhlmann, J., Diese, J., Dreizler, S., Hessman, F. V., Husser, T.-O., Miller, G. F., Nickol, N., Pons, R., Ruhr, D., et al., 2011, A&A 526, 53
- Beuermann, K., Hessman, F. V., Dreizler, S., Marsh, T. R., Parsons, S. G., Winget, D. E., Miller, G. F., Schreiber, M. R., Kley, W., Dhillon, V. S., et al., 2011b, 2010, A&A, 521, L60
- Brinkworth, C. S., Marsh, T. R., Dhillon, V. S., Knigge, C., 2006, MNRAS 365, 287
- Bruch, A., 1999, AJ, 117, 3031
- Bruch, A. & Diaz, M. P. 1998, AJ, 116, 908
- Doyle, L. R., Carter, J. A., Fabrycky, D. C., et al., 2011, Science 333, 1602.
- Hinse, T. C., Lee, J. W., Gozdzewski, K., et al., 2011, arXiv: 1112.0066.
- Horner, J., Marshall, J. P., Wittenmyer, R. A., Tinney, C. G., 2011, MNRAS 416, L11
- Krzeminski, W. 1984, IAU Circ. 4014
- Maxted, P. F. L., Marsh, T. R., Morales-Rueda, L., Barstow, M. A., Dobbie, P. D., Schreiber, M. R., Dhillon, V. S., Brinkworth, C. S., 2004, MNRAS 355, 1143
- Maxted, P. F. L., O'Donoghue, D., Morales-Rueda, L., Napiwotzki, R., Smalley, B., 2007, MNRAS 376, 919
- O'Brien, M. S., Bond, H. E., Sion, E. M., 2001, ApJ 563, 971
- O'Donoghue, D., Koen, C., Kilkeny, D., Stobie, R. S., Koester, D., Bessell, M. S., Hambly, N., MacGillivray, H., 2003, MNRAS 345, 506
- Parsons, S. G., Marsh, T. R., Copperwheat, C. M., Dhillon, V. S., Littlefair, S. P., et al., 2010, MNRAS 407, 2362
- Qian, S.-B., Dai, Z.-B., Liao, W.-P., Zhu, L.-Y., Liu, L., Zhao, E. G., 2009, ApJ 706, L96
- Qian, S.-B., Liao, W.-P., Zhu, L.-Y., Dai, Z.-B., 2010a, ApJ 708, L66
- Qian, S.-B., Liao, W.-P., Zhu, L.-Y., Dai, Z.-B., Liu, L., He, J.-J., Zhao, E.-G., and Li, L.-J., 2010b, MNRAS 401, L34
- Qian S.-B., Liu, L., Liao, W.-P., Li, L.-J., Zhu, L.-Y., Dai, Z.-B., He, J.-J., Zhao, E.-G., Zhang, J., and Li, K., 2011, MNRAS 414, L16
- Qian S.-B., Zhu L.-Y., Dai Z.-B., Fernández Lajús, E., Xiang F.-Y., and He, J.-J., 2012, ApJ 745, L23
- Stumpff, P., 1980, A&AS 41, 1
- Wittenmyer, R. A., Horner, J., Marshall, J. P., Butters, O. W., Tinney, C. G., 2012, MNRAS 419, 3258
- Zuckerman, B., Koester, D., Reid, I. N., Hünsch, M., 2003, ApJ 596, 477